On the Origin of the Tropical Intraseasonal Oscillation*

WINSTON C. CHAO

Atmospheric Chemistry and Dynamics Branch, Laboratory for Atmospheres, NASA/Goddard Space Flight Center, Greenbelt, MD 20771

(Manuscript received 22 August 1986, in final form 12 January 1987)

ABSTRACT

This study provides an explanation for the origin of the tropical intraseasonal (40–50 day) oscillation (TIO) based on a simple generalization of Gill's linear analytic model for tropical large-scale heat-induced circulation. The solution, which compares favorably with observations, contains a convective region that excites an eastward-moving Kelvin wave and a westward-moving Rossby wave. The significance of the Rossby wave, not previously emphasized, is clearly revealed. The entire system moves eastward as a response to the circulation it excites at a speed at which the latent heat energy in the tropics is best extracted. Thus, the TIO is viewed as an intrinsic instability. Its speed is related to the vertical heating profile and is a decreasing function of both dissipation and the zonal size of the convective region. This speed is a weighted mean of the speed of the Kelvin wave and that of the Rossby wave. Previous studies have erroneously equated the speed of the TIO with that of the Kelvin wave. This study also demonstrates that classification of the TIO as a wavenumber 1 phenomenon is not advisable.

1. Introduction

The tropical intraseasonal oscillation (TIO) in the troposphere was discovered by Madden and Julian (1971, 1972), among others. In the vertical plane along the equator, the flow structure of this phenomenon (Fig. 1) encompasses a convective region on the order of 6000–9000 km associated with upward motion. Outside the convective region exists a compensatory downward motion that extends both eastward and westward. In the entire zonal belt, there is only one convective region associated with TIO, and the whole pattern travels eastward relative to both the earth's surface and the basic flow. The speed corresponds to a periodicity of approximately 30 to 80 days, although the name "40–50 day wave" is often used. The variation in speed is to some extent explained by the variation in speed of the basic flow. The traveling convective region associated with TIO, which is perennial and subject to seasonal variation, has been observed mainly in the Indian Ocean and in the Western and Central Pacific, where sea surface temperatures are higher than in other regions.

The zonal wind perturbations associated with the TIO exhibit an out-of-phase relationship in the upper and lower troposphere; i.e., a baroclinic structure. A negative sea-level pressure perturbation is found near the convective region, and low-level zonal wind convergence is in phase with upward motion. The meridional wind perturbation, if it exists, is much smaller than the zonal component. The TIO is confined in the tropics and has its largest amplitude between 10°S and 10°N. Oscillations of similar periodicity, which may be interacting with the TIO, have been observed in the middle latitudes, but they are believed to have different origins (Lau and Phillips, 1986).

The TIO has been tied to variations in the Indian monsoon (Murakami and Nakazawa, 1985; Yasunari, 1980, 1981), and to the variation in the Mei-Yu regime over South China (Lau and Chan, 1986). Furthermore, a link to the El Niño/Southern Oscillation has been proposed (Lau, 1985).

Previous attempts to explain the TIO have not been completely satisfactory. Chang's (1977) study pointed out the crucial roles played by the Kelvin wave and by viscosity (also see comments by Stevens and White, 1979). However, in Chang's study, no consideration was given to the other types of waves, i.e., the mixed Rossby–gravity wave and the Rossby waves excited by the convection. Subsequently Yamagata and Hayashi's (1984) study avoided that problem, but it called for an externally imposed periodicity of 40–50 days in the convective heating without providing any justification. Other studies also failed to furnish a complete explanation for the TIO. Recently Lau and Peng (1987) performed a numerical study that complements our study. However, like earlier studies, their equating of the speed of the TIO to that of a low-speed internal Kelvin wave is contrary to our findings. Hayashi and Sumi (1986) also successfully simulated TIO with a simplified GCM. Their results, along with those of Lau and Peng, can be better understood with the help of our study.

With the aid of an analytic model, this study offers an explanation for the TIO. The basic concept is pre-

* Contribution Number 42 of the Stratospheric General Circulation with Chemistry Modeling Project, NASA/GSFC.

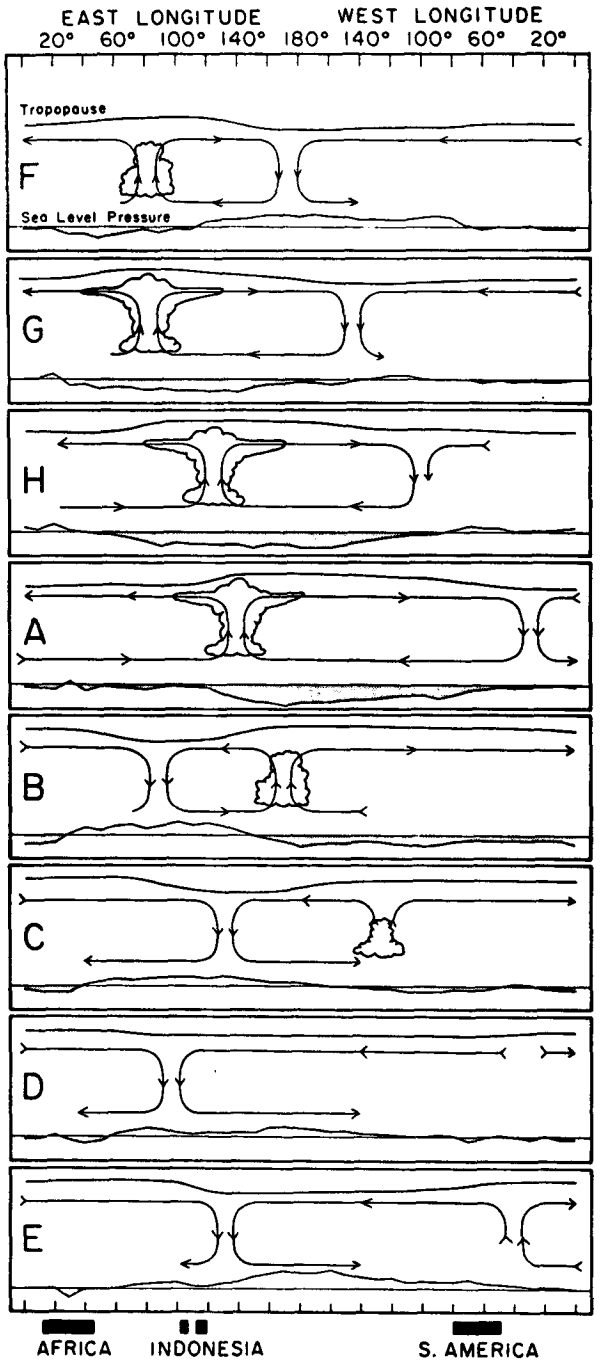

FIG. 1. Schematic depiction of the time and space (zonal plane) variations of the circulation cells associated with the 40–50 day oscillation. The mean pressure disturbance is plotted at the bottom of each chart with negative anomalies shaded. Regions of enhanced large-scale convection are indicated schematically by the cumulus and cumulonimbus clouds. The relative tropopause height is indicated at the top of each chart. (From Madden and Julian, 1972.)

sented in section 2. Section 3 describes the analytic model and the method of solution. The solution of the model and its comparison with observations are presented in section 4. Discussion and summation of the results comprise the final section.

2. The basic concept

Gill's (1980) analytic study forms the foundation of our effort; therefore, a recapitulation of his work is in order. Briefly, Gill made a linear study of the steady tropical circulation forced by a large-scale stationary convective heat source—representing the maritime continent—on an equatorial β-plane. The basic state is at rest. In the vertical directions only one mode—the most fundamental baroclinic mode in the troposphere—is considered. Thus, the governing equations can be reduced to the forced shallow-water equations. Damping is treated by simple Rayleigh friction and Newtonian cooling. For mathematical convenience, the damping coefficient for friction is assumed to be the same as that for cooling. This assumption is, of course, arguable. Furthermore, only steady-state solutions are sought, and stationary heating is prescribed in a limited domain (40° in the longitudinal direction).

Gill obtained solutions for symmetric (with respect to the equator) and antisymmetric heating cases. With symmetric heating, the solution has two parts. One part is a circulation in the convective region to its east, identified as eastward-moving Kelvin wave. The other part is a circulation in the convective region to its west, identified as a westward-moving long planetary (Rossby) wave traveling at a speed one-third that of the Kelvin wave. When the heating is antisymmetric, no Kelvin wave is excited and circulation exists only in the heating region and to its west. When the solutions for symmetric and antisymmetric forcing are combined, the resulting circulation bears a remarkable resemblance to the observed seasonal mean circulation around the maritime continent. Nonlinear advective terms ignored in this linear study were later found not to be qualitatively important (Gill and Philips, 1986).

The present study embodies a generalization of Gill's work. Instead of studying tropical circulation induced by a prescribed *stationary* heat source, we shall study circulation induced by a heat source of the same strength and spatial structure *traveling* at a constant speed, C_0. In terms of the flow converging into the convective region, the response to this traveling heat source as a function of C_0 is maximum (i.e., there is a resonant response) at a particular C_0, $\hat{C}_0$. Basically, when the heat source, with its intensity fixed, is not anchored by the maritime continent and is allowed to travel as a response to the heat induced circulation, it is pulled by the Kelvin wave toward the east and by the Rossby wave toward the west. Thus, the convective region travels with a weighted mean speed, somewhere between the speeds of Kelvin and Rossby waves. This weighted mean speed must be eastward because of the greater speed and stronger divergence field of the Kelvin wave. The precise determination of this speed necessitates the following dynamical consideration.

If the strength of the convective heating, rather than being prescribed, is sustained by the moisture flux convergence in the lower atmosphere [as in the study of conditional instability of the second kind, (CISK)], then the convective region and the whole perturbation structure associated with it should travel at a speed of $\hat{C}_0$. At this speed, the whole perturbation structure is optimally capable of tapping into the latent heat energy in the tropics, and thus is least apt to be dissipated. Within the scope of our simple model, we contend that this perturbation structure, moving with a speed of $\hat{C}_0$, can be equated with the observed TIO. Thus, we view the TIO as an instability intrinsic to the tropics. This concept is developed in the following sections by solving for $\hat{C}_0$ and the corresponding perturbation structure. The solutions are then compared with the observational data.

3. The governing equations and the method of solution

Since our governing equations are basically taken from Gill (1980), the derivations of these equations will not be repeated here. Only the changes will be discussed. (See Geisler and Stevens, 1982, for a discussion of the vertical structure of Gill's model.) The sole modification of Gill's equations that we have made was a generalization: namely, that instead of being stationary, the heat source travels in the zonal direction at a constant prescribed speed, C_0. The equations are written in a frame of reference that travels with the heat source—i.e., the heat source is stationary; the steady-state solution is sought. These equations take the form of linearized and forced shallow water equations on an equatorial β-plane. In nondimensional form they are

$$-C_0\frac{\partial u}{\partial x}+\epsilon(u+C_0)-\frac{1}{2}yv=-\frac{\partial p}{\partial x}, \tag{1}$$

$$\frac{1}{2}y(u+C_0)=-\frac{\partial p}{\partial y}, \tag{2}$$

$$-C_0\frac{\partial p}{\partial x}+\epsilon p+\frac{\partial u}{\partial x}+\frac{\partial v}{\partial y}=-Q, \tag{3}$$

$$-w=\frac{\partial u}{\partial x}+\frac{\partial v}{\partial y}. \tag{4}$$

From these equations, it is evident that the basic state is at rest with respect to the earth's surface; $u = -C_0$ when there is no perturbation. These equations reduce to those of Gill, of course, when $C_0 = 0$. In these equations, time and length have been scaled by $(2\beta c)^{-1/2}$ and $[c/(2\beta)]^{1/2}$, respectively, where $c \equiv (gH)^{1/2}$, g is the acceleration due to gravity, and H is the equivalent depth. Here p is proportional to the pressure perturbation and x and y are the eastward and northward distances, respectively. The coordinate frame moves eastward along the equator with a nondimensional speed of C_0 with respect to the earth's surface. Since $u + C_0$ is the zonal speed with respect to the earth's surface, Eq. (2) retains the "long wave" approximation in the zonal direction invoked by Gill. [Eq. (2) is thus identical to Eq. (2.12) of Gill, 1980. For a discussion of this approximation, see Lim and Chang, 1983.] ϵ is the nondimensional dissipation rate. The boundary conditions are

$$u+C_0=p=v=0, \quad \text{as} \quad |x| \text{ or } |y| \to \infty.$$

The solutions to the shallow water equations (1)–(4), $u + C_0$, v, and p, can be viewed as solutions, in the resting coordinate frame, in the lower level of a two-level model. In the upper level, the solutions in the resting coordinate frame are $-(u + C_0)$, $-v$ and $-p$.

The method of solution is identical to that of Gill (1980). To facilitate the solution, two new variables, q and r, are introduced:

$$q=p+(u+C_0)$$

$$r=p-(u+C_0).$$

The sum and difference of (1) and (2) give

$$-C_0\frac{\partial q}{\partial x}+\epsilon q+\frac{\partial q}{\partial x}+\frac{\partial v}{\partial y}-\frac{1}{2}yv=-Q \tag{5}$$

$$-C_0\frac{\partial r}{\partial x}+\epsilon r-\frac{\partial r}{\partial x}+\frac{\partial v}{\partial y}+\frac{1}{2}yv=-Q, \tag{6}$$

respectively, and (2) can be rewritten as

$$\frac{\partial q}{\partial y}+\frac{\partial r}{\partial y}+\frac{1}{2}y(q-r)=0. \tag{7}$$

Variables q, r, v and Q are expanded in terms of parabolic cylinder functions, $D_n(y)$, which are the free solutions of (5), (6) and (7). Thus

$$q=\sum_{n=0}^{\infty} q_n(x)D_n(y),$$

etc. Given

$$\frac{dD_n}{dy}+\frac{1}{2}yD_n=nD_{n-1}$$

$$\frac{dD_n}{dy}-\frac{1}{2}yD_n=-D_{n+1},$$

(5)–(7) yield

$$\left.\begin{aligned}(1-C_0)\frac{dq_0}{dx}+\epsilon q_0&=-Q_0\\ (1-C_0)\frac{dq_{n+1}}{dx}+\epsilon q_n-v_n&=-Q_{n+1}, \quad n\geq 0\end{aligned}\right\} \tag{8}$$

$$-(1+C_0)\frac{dr_{n-1}}{dx}+\epsilon r_{n-1}+nv_n=-Q_{n-1}, \quad n\geq 1 \tag{9}$$

$$\left.\begin{aligned}q_1&=0\\ r_{n-1}&=(n+1)q_{n+1}, n\geq 1\end{aligned}\right\}. \tag{10}$$

As in Gill (1980), two types of heating functions can render simple solutions. The first instance, the heating rate, Q, is symmetric about the equator and has the form

$$Q(x,y) = F(x)D_0(y) = F(x)\exp\left(-\tfrac{1}{4}y^2\right).$$

In the second case, Q is antisymmetric about the equator and has the form

$$Q(x,y) = F(x)D_1(y) = F(x)y\exp\left(-\tfrac{1}{4}y^2\right).$$

These simple heating functions allow the solutions to be expressed by only the first four D_ns, which are

$$D_0, D_1, D_2, D_3 = (1, y, y^2-1, y^3-3y)\exp\left(-\tfrac{1}{4}y^2\right).$$

The zonal dependence of Q has the form

$$F(x) = \begin{cases} \cos(kx), & |x| < L \\ 0, & |x| > L, \end{cases}$$

where $k = \pi/(2L)$, and L is the half-zonal width of the convective region. Our primary focus is the symmetric heating case.

4. The solution and its comparison with observations

With symmetric forcing, the solution has different forms for $C_0 > 1$ and $C_0 \leqslant 1$. The solution for $C_0 > 1$ is not important to our discussion and is, therefore, not presented. When $C_0 \leqslant 1$, (8)–(10) have the following first part of the solution:

$$[k^2(1-C_0)^2+\epsilon^2]q_0 = \begin{cases} 0, & x<-L \quad (11a) \\ -\epsilon\cos(kx) - (1-C_0)k\left[\sin(kx) + \exp\left\{\dfrac{-\epsilon}{(1-C_0)}(x+L)\right\}\right], & |x|<L \quad (11b) \\ -k(1-C_0)\left\{1+\exp\left(\dfrac{-2\epsilon L}{(1-C_0)}\right)\right\}\exp\left[\dfrac{-\epsilon_1}{(1-C_0)}(x-L)\right], & x>L. \quad (11c) \end{cases}$$

The associated perturbation fields are

$$\left.\begin{aligned} p = u + C_0 &= \tfrac{1}{2}q_0(x)\exp\left(-\tfrac{1}{4}y^2\right) \\ v &= 0 \end{aligned}\right\}. \quad (12)$$

The foregoing equations represent a stationary forced Kelvin wave that diminishes eastwards. If F and ϵ are suddenly changed to zero, this perturbation will progress eastward with a speed of $(1 - C_0)$ with respect to the moving frame of reference. Equation (11a) indicates that no perturbation exists west of the heat source.

The other part of the solution is

$$[k^2(1-C_0)^2+9\epsilon^2]q_2 = \begin{cases} -(1-C_0)k\left[1+\exp\left\{\dfrac{-6\epsilon L}{(1-C_0)}\right\}\right]\exp\left\{\dfrac{3\epsilon_1}{(1-C_0)}(x+L)\right\}, & x<-L \quad (13a) \\ -3\epsilon\cos(kx) + (1-C_0)k\left[\sin(kx) - \exp\left\{\dfrac{3\epsilon}{(1-C_0)}(x-L)\right\}\right], & |x|<L \quad (13b) \\ 0, & x>L. \quad (13c) \end{cases}$$

The associated perturbation fields are

$$\left.\begin{aligned} p &= \tfrac{1}{2}q_2(y^2+1)\exp\left(-\tfrac{1}{4}y^2\right) \\ u + C_0 &= \tfrac{1}{2}q_2(y^2-3)\exp\left(-\tfrac{1}{4}y^2\right) \\ v &= (F+4\epsilon q_2)y\exp\left(-\tfrac{1}{4}y^2\right) \end{aligned}\right\}. \quad (14)$$

The foregoing equations represent a stationary forced Rossby wave that diminishes westward with a spatial decay rate of $3\epsilon_1/(1 - C_0)$, which is three times that of q_0. If F and ϵ are suddenly changed to zero, this perturbation will propagate westward with a speed of $(1 - C_0)/3$ with respect to the moving frame. The combination of the Kelvin and the Rossby components gives the TIO solution. For the special case of $C_0 = 1$, no perturbation exists outside the convective region. In addition, we have allowed the dissipation rate outside the convective region to assume a smaller value,

ϵ_1, than inside the convective region. However, as the following discussion will show, ϵ_1 does not affect the speed selection. Thus, all the results will be given with $\epsilon_1 = \epsilon$.

The total perturbation eddy energy is proportional to E, where

$$E \equiv \int_{-\infty}^{\infty}\int_{-\infty}^{\infty} \frac{1}{2}[(u+C_0)^2+v^2+p^2]dxdy.$$

Ordinarily, in a linear resonance study where heating is completely prescribed externally, the resonant C_0 is the C_0 that gives the maximum E. Here, however, we are more interested in the feedback case where convective heating is favored by larger moisture convergence. Thus, as already mentioned in section 2, we will define $\hat{C}_0$ as the C_0 that maximizes the horizontal moisture convergence in a region surrounding the core of the prescribed convective region. The horizontal moisture convergence in the convective region is proportional to

$$W \equiv \int_{-1}^{1}\int_{-L/2}^{L/2} w dxdy,$$

where the size of the integration domain is somewhat arbitrarily set. Changing the integral x domain from $\pm L/2$ to $\pm L$ does not change $\hat{C}_0$ significantly, nor does changing the integral y domain from ± 1 to ± 2. Of course, the supply of moisture depends not only on convergence but also on evaporation in the convective region. However, the latter is a much smaller factor and is thus not taken into account in our simple model.

An example of W as a function of C_0 is given in Fig. 2. The $\hat{C}_0$, numerically determined as a function of L and ϵ, is shown in Fig. 3 and is a decreasing function of both ϵ and L. This dependence of $\hat{C}_0$ on ϵ can be traced to the fact that the governing equations for both q_0 and q_2, Eq. (8), have a ratio factor of $\epsilon/(1 - C_0)$. Thus, when ϵ is increased, in order to keep the solution least affected C_0 (and therefore $\hat{C}_0$) has to decrease. The dependence of $\hat{C}_0$ on L can be seen from the fact that L is multiplied by ϵ in (11) and (13), and thus increasing L has a similar effect as increasing ϵ.

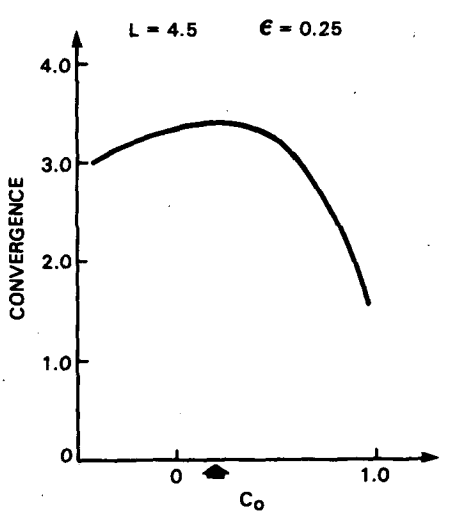

FIG. 2. W as a function of C_0 for $L = 4.5$ and $\epsilon = 0.25$. The arrow indicates $\hat{C}_0$.

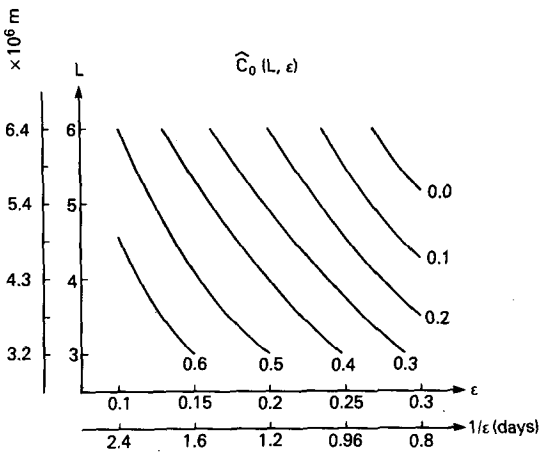

FIG. 3. The nondimensional TIO speed $\hat{C}_0$ as a function of the nondimensional size of the convective region, L, and the nondimensional rate of dissipation, ϵ. $\hat{C}_0$ should be multiplied by c ($\sim$50 m s^{-1}) to yield its dimensional value. Dimensional L and $1/\epsilon$ are shown on separate scales.

When comparing our results with observations, it is necessary to set a few scaling parameters. The precise choice of these parameters is not easy. However, our goal is to demonstrate that with suitable choices of these parameters, our results correspond reasonably well with observations. The choice for c reported in the literature varies from 30 to 80 m s^{-1}. We chose $c = 50$ m s^{-1} after Fulton and Schubert (1985). This choice sets the length scale, $(c/2\beta)^{1/2}$, at $\sim 1.07 \times 10^6$ m, and the time scale, $(2\beta c)^{-1/2}$, at $\sim 0.215 \times 10^5$ s. Holton and Colton (1972) used a large dissipation coefficient of 1.5×10^{-5} s^{-1} for their vorticity equation to get good quantitative results, and we will approximately follow their choice and use a dissipation coefficient of 1.2×10^{-5} s^{-1}, which sets ϵ at 0.25. It should be emphasized that this large dissipation coefficient needs to be applied only in the convective region. Outside the convective region, a much smaller ϵ, ϵ_1, can be used without affecting $\hat{C}_0$. We also chose $L = 4.5$. The observed L varies from 2 to 6 (Fig. 4 of Knutson et al., 1986). These parameter settings yield a $\hat{C}_0$ of 0.2, which in dimensional form is $\sim$10 m s^{-1}. This speed compares very favorably with the observed TIO speed of 3–6 m s^{-1} in the Indian Ocean and in the Western Pacific when a typical low-level basic wind speed of -5 m s^{-1} is assumed.

The perturbation fields computed with our choices for L and ϵ are shown in Fig. 4. The wind field in Fig. 4 is relative to the earth's surface, and the wind direc-

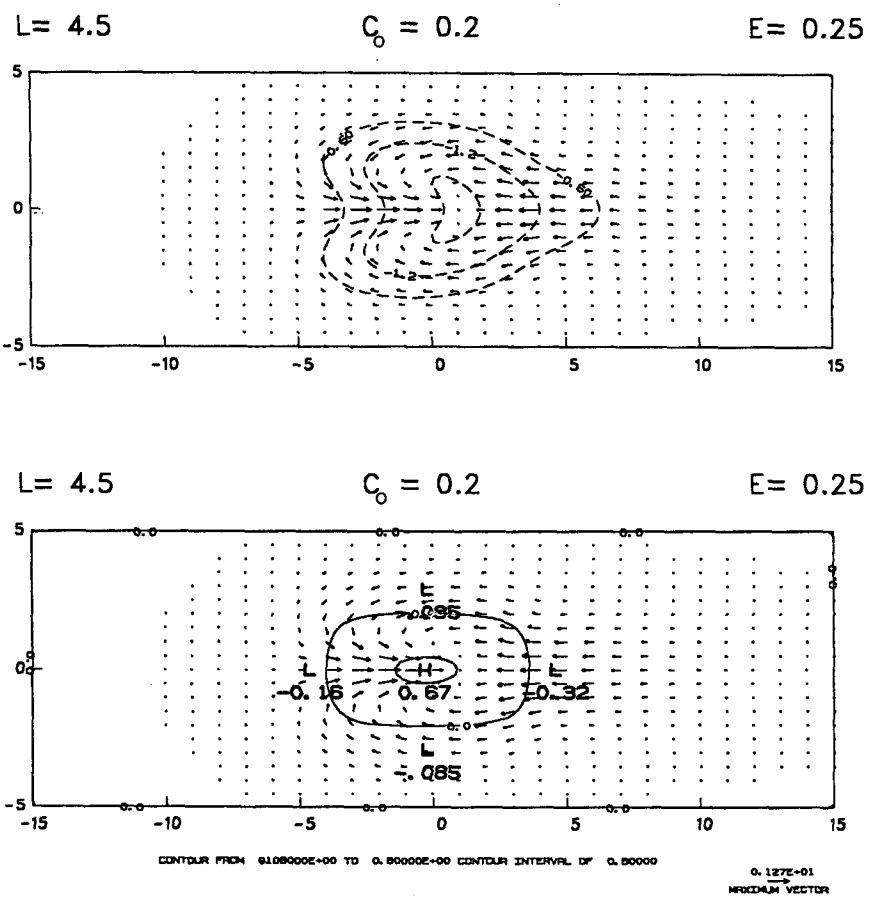

FIG. 4. Horizontal distribution of pressure perturbation (upper) and vertical velocity (lower) superimposed on wind arrows relative to the earth's surface for $L = 4.5$, $\epsilon = 0.25$ and $C_0 = 0.2$. All quantities are nondimensional.

tion is mostly zonal, in accordance with observations. It should be emphasized, however, that the meridional wind, though small, is not zero for $x < L$, indicating that the Rossby wave makes a significant contribution to the TIO. The existence of the Rossby wave has been shown in the recent observational study (Madden,

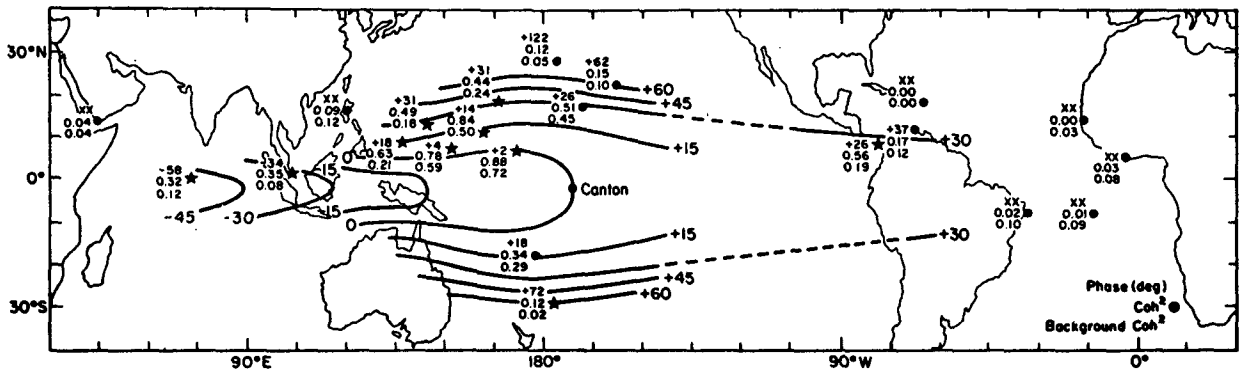

FIG. 5. Mean phase angles, coherence-squares for approximately the 36–50-day period range of cross spectra between all stations and Canton. The plotting model is given in lower right-hand corner. Positive phase angles at a station means the Canton series leads that of the station. Stations indicated by a star have coherence-squares above the background at the 95% level. Mean coherence-squares at Shemya (52°43'N, 174°6'E) and Campbell Island (52°33'S, 169°9'E) (not shown) are 0.08 and 0.02, respectively. Both are below their average background coherence-squares. (From Madden and Julian, 1972.)

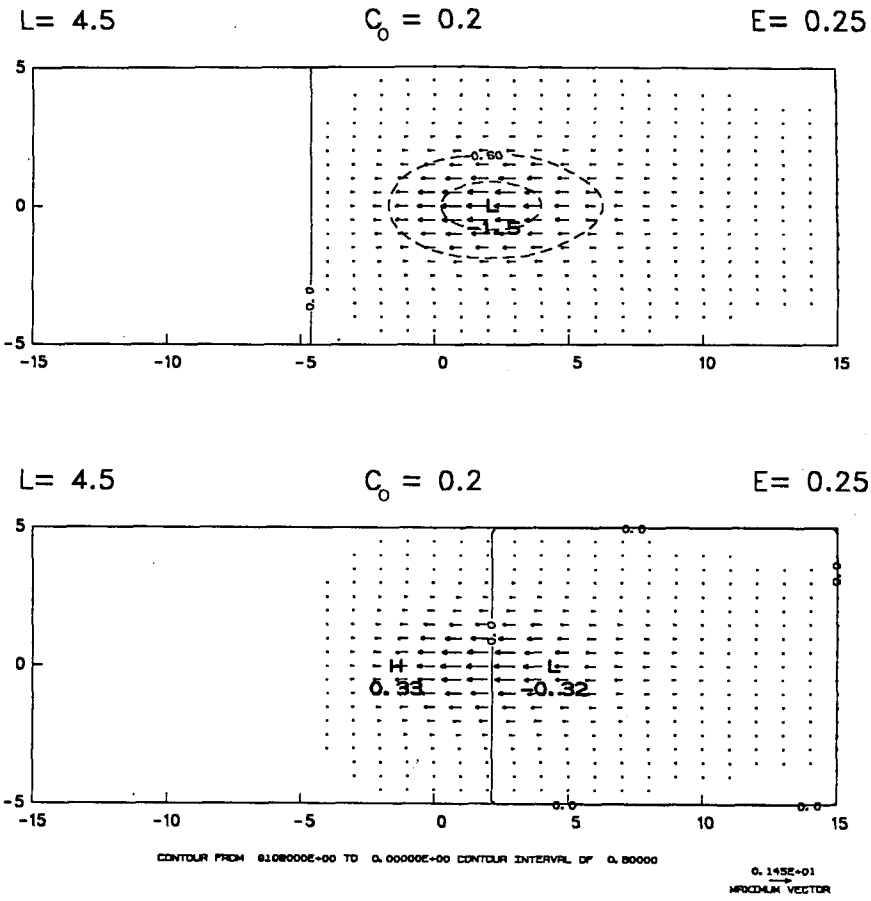

FIG. 6. The Kelvin wave component of Fig. 4.

1986). Also, two downward compensating motion centers (implying two vertical circulation cells along equator) appear on the east and west sides of the convective region due to the Kelvin wave and to the Rossby wave, respectively.

Figure 4 shows that the downward compensating motion center is larger east of the convective region than west of the region. The downward motion center west of the convective region, though smaller than the one east of the convection region, is nonetheless sizable, again indicating that the Rossby wave is a significant component of the TIO.

Examination of the phase angle distribution of the sea level pressure perturbation provides another way of comparing our results with observations. Madden and Julian's (1972) observed phase angle of the sea-level pressure perturbation associated with the TIO (Fig. 5) shows that across the equator, the constant phase lines change their orientation from NW–SE north of the equator to NE–SW south of the equator. This supports our results in that if a line is drawn in Fig. 4 for $\partial p/\partial x = 0$ as a function of x and y, it shows the same change of orientation across the equator. Figures 6 and 7 show the Kelvin wave and Rossby wave components of Fig. 4, respectively. Both components have a $\partial p/\partial x = 0$ line in the north–south direction. This is also evident from (12) and (14). Therefore, the orientation of the $\partial p/\partial x = 0$ line in Fig. 4 is clearly due to the superposition of the two components. In contrast, Chang's (1977) results showed that the meridional phase change depended on the growth rate of the tropospheric Kelvin wave, which he interpreted as the TIO. The observed TIO, however, is rather steady and has no sizeable growth rate. Further comparisons could be made if a composite study of the observed horizontal structure of the TIO had been done.

5. Discussion and summary

One important remaining problem is how L is determined. Related to this problem is the determination of zonal size of the OLR dipole structure. For a given ϵ, $\hat{C}_0$ is a function of L; thus, one can determine the ratio of convergence to total heating in the convective region at $C_0 = \hat{C}_0$ as a function of L. Our calculation shows that this ratio is a decreasing function of L and has a maximum at $L = 0$. This result is consistent with Lau and Peng's (1987) numerical simulation results

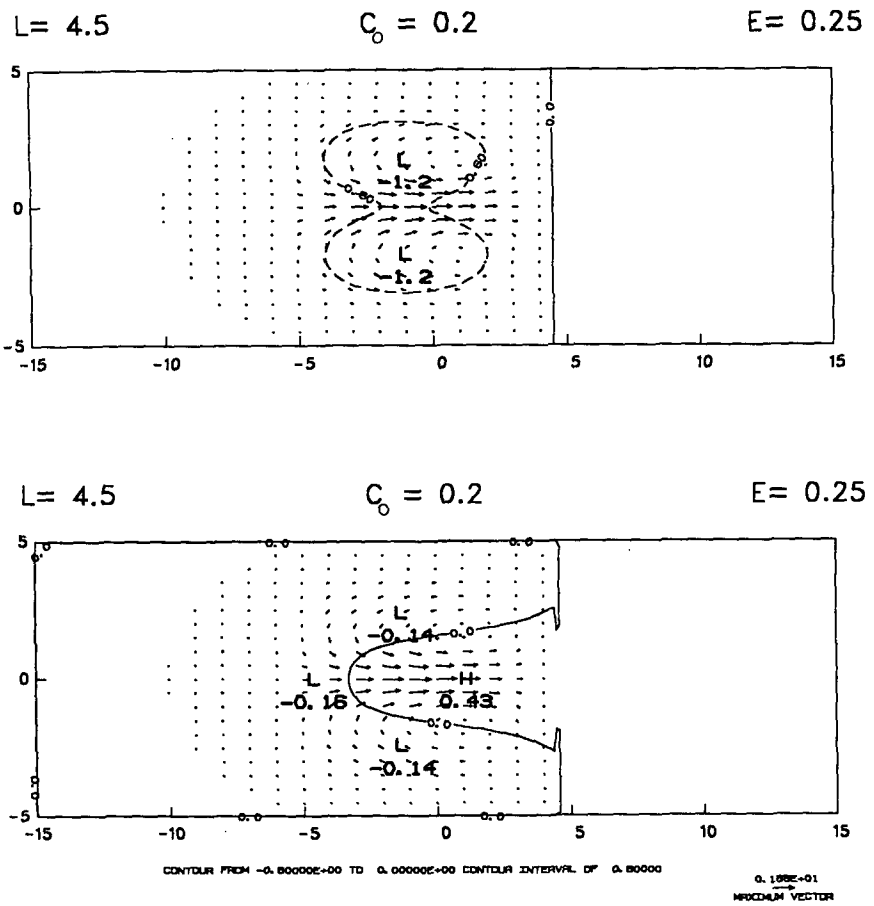

FIG. 7. The Rossby wave component of Fig. 4.

that show a convective region of a size corresponding to that of the highest resolvable wavenumber in their spectral model. This problem is precisely the same problem that has been encountered in the study of conditional instability of the second kind (CISK). For this, Chao (1979) proposed a possible solution described below.

In the study of CISK, the heating function is often expressed as

$$Q \propto \eta(p)\omega\bar{q}$$

where ω and $\bar{q}$ are the vertical velocity and the water vapor mixing ratio at the top of the boundary layer, respectively, and $\eta(p)$ is a vertical distribution function whose vertical integral is unity. Chao's (1979) study showed that when $\eta(p)$ is independent of the horizontal size of the disturbance, l, the CISK growth rate is maximum at the smallest l. On the other hand, if $\eta(p)$ is a function of l (this can be achieved, for example, through a cumulus parameterization scheme that depends on the entire vertical profile of the vertical velocity), the CISK growth rate is maximum at a more realistic l.

The average periodicity of 45 days for the TIO is equivalent to an average speed of 10 m s^{-1}. The fact that the TIO has an average speed of 3 to 6 m s^{-1} in the Indian Ocean and in the Western Pacific (50°–160°E) (Knutson et al., 1986, Fig. 5) implies that the average speed elsewhere along the equator must be much greater than 10 m s^{-1}. Although the basic wind may aid the TIO in attaining a faster eastward speed, it does not provide a complete explanation for the speed differences along the equator. Here we propose another possibility. Because of the relatively cold sea surface temperatures in the eastern Pacific and in the eastern Atlantic, little or no convective heating is provided there. The TIO traveling into these regions would then dissipate at a rate of ϵ_1, which is much smaller than ϵ. The propagation characteristics of the disturbance would also change. In our simple model, if the convective heating is cut off within a period less than the dissipation time scale associated with ϵ_1, the disturbance would disintegrate into two components: the Kelvin wave and the Rossby wave—each propagating in different directions at its own speed relative to the basic flow. The eastward-moving component, the Kelvin wave, would have a speed c much larger than that of the original disturbance. This greater eastward speed combined with the smaller dissipating rate ϵ_1 would

prevent the disturbance from being completely dissipated before it could reach another latent-heat-rich region. Another, perhaps more likely possibility is that as the convective region diminishes in the eastern Pacific, the subsiding vertical motion over the Indian Ocean, which inhibits convection, also diminishes. Thus, another convective region can form in the Indian Ocean. In this scenario the TIO does not travel all the way around the globe.

On the equatorial vertical plane, the downward motion associated with TIO is largest immediately outside of the convective region. Further away from the convective region the downward vertical motion diminishes exponentially. This phenomenon exists in many other types of circulation in the tropics. The best example is the well-known clearest sky surrounding tropical cyclones. Another example is the minimum just to the north and south of ITCZ in seasonal mean cloudiness pictures.

The observational fact that only one convective region associated with the TIO exists in the entire tropical belt needs to be considered. If there were more than one, all the convective regions would be in downward branches of vertical circulation cells induced by other convection regions, and would therefore be suppressed. Thus, a single convective region is the most preferred mode. This preference can also be explained by considering a situation where two convective regions on the equator in a two-level model are given initially. The associated circulation in the lower level in this situation is the self-superposition of Fig. 4 with an east–west shift. Thus, each convective region is drawn toward the other by the inflow associated with the other. Consequently, the two convective regions will eventually coalesce if one of them is not already annihilated by the other. In this argument the flows in the upper level, not affecting the moisture convergence, play a passive role. By the same reasoning, one can conclude that the whole TIO perturbation pattern will not disintegrate into two parts despite the pulling of the Kelvin and Rossby waves in the opposite directions. The fact that only a single convective region exists does not imply the disturbance is a wavenumber 1 phenomenon, though wavenumber 1 is an important component. Rather, classification of the TIO as a wavenumber 1 phenomenon would require a sinusoidal zonal distribution of the perturbation fields, which clearly contradicts observations.

The large choice of damping coefficient deemed necessary by Holton and Colton (1972), which we have adopted, has been demonstrated by Sardeshmukh and Held (1984) to be, to certain extent, due to nonlinearity. The relative importance of cumulus friction and nonlinearity in providing damping remains to be determined. The importance of the nonlinear terms may explain the fact that the TIO speed diminished with increasing horizontal resolution in the GFDL GCM (Lau and Lau, 1986).

The importance of the vertical profile of the convective heating in determining c has been indicated in numerous studies (e.g., Fulton and Schubert, 1985). Consequently, a realistic cumulus parameterization is very important in obtaining reasonable TIO speed in general circulation models. Moreover, the dependence of $\hat{C}_0$ on ϵ indicates that nonlinearity and the precise treatment of dissipation (e.g., cumulus friction) are also crucial for TIO in GCMs.

In summary, the basic characteristics of TIO can be understood with the aid of a simple generalization of Gill's analytic model. The speed of TIO is a weighted mean of the speeds of the Kelvin and Rossby waves. We contend that this speed is the one at which the moisture convergence into the convective region has a maximum. Thus, we view the TIO as an intrinsic instability in the tropics. The speed of TIO is related to the vertical heating profile and is a decreasing function of both the dissipation (including nonlinearity) and zonal size of the convective region. The TIO perturbation structure in our solution compares favorably with observations in the following ways: 1) the perturbation winds are mainly in the zonal direction; 2) the largest negative surface pressure perturbation is situated close to the center of the convective region; 3) the phase change in the meridional direction of the pressure field (due to the superposition of the Kelvin wave and the Rossby wave) is realistic; 4) with a suitable choice of model parameters, a realistic TIO speed is obtained; and 5) the two parts of the solution, the Kelvin wave and the Rossby wave, give rise to the vertical circulation cells on the east and west sides of the convective region, respectively.

Finally, the two most important contributions of the present work are 1) the speed and the horizontal structure of the TIO can be understood by a simple generalization of Gill's analytic model and 2) the significance of the Rossby wave, not previously emphasized, has been clearly demonstrated.

REFERENCES

Chang, C. P., 1977: Viscous internal gravity waves and low-frequency oscillations in the tropics. *J. Atmos. Sci.*, **34**, 901–910.

Chao, W. C., 1979: A study of conditional instability of the second kind and a numerical simulation of the intertropical convergence zone and easterly waves. Ph.D. dissertation, UCLA. 253 pp.

Fulton, S. R., and W. H. Schubert, 1985: Vertical normal mode transforms: Theory and application. *Mon. Wea. Rev.*, **113**, 647–658.

Geisler, J. E., and D. E. Stevens, 1982: On the vertical structure of damped steady circulation in the tropics. *Quart. J. Roy. Meteor. Soc.*, **108**, 87–93.

Gill, A. E., 1980: Some simple solutions for heat induced tropical circulation. *Quart. J. Roy. Meteor. Soc.*, **106**, 447–462.

——, and P. J. Philips, 1986: Nonlinear effects on heat-induced circulation of the tropical atmosphere. *Quart. J. Roy. Meteor. Soc.*, **112**, 69–91.

Hayashi, Y.-Y., and A. Sumi, 1986: The 30–40 day oscillations simulated in an "aqua planet" model. *J. Meteor. Soc. Japan.*, **64**, 451–467.

Holton, J. R., and D. E. Colton, 1972: A diagnostic study of the

vorticity balance at 200 mb in the tropics during the northern summer. *J. Atmos. Sci.*, **29,** 1124–1128.

Knutson, T. R., K. M. Weickmann and J. E. Kutzbach, 1986: Global-scale intraseasonal oscillations of outgoing longwave radiation and 250 mb zonal wind during Northern Hemisphere summer. *Mon. Wea. Rev.*, **114,** 605–623.

Lau, K.-M., 1985: Elements of a stochastic-dynamical theory of the long-term variability of the El Niño/Southern Oscillation. *J. Atmos. Sci.*, **42,** 1552–1558.

——, and P. H. Chan, 1985: Aspects of the 40–50 day oscillation during the northern winter as inferred from outgoing longwave radiation. *Mon. Wea. Rev.*, **113,** 1889–1909.

——, and L. Peng, 1987: Origin of low-frequency (intraseasonal) oscillations in the tropical atmosphere. Part I: The basic theory. *J. Atmos. Sci.*, **44,** 950–972.

——, and T. J. Phillips, 1986: Coherent fluctuations of extratropical geopotential height and tropical convection in intraseasonal time scales. *J. Atmos. Sci.*, **43,** 1169–1181.

Lau, N. C., and K. M. Lau, 1986: Structure and propagation of intraseasonal oscillations appearing in a GFDL GCM. *J. Atmos. Sci.*, **43,** 2023–2047.

Lim, H., and C. P. Chang, 1983: Dynamics of teleconnections and Walker circulation forced by equatorial heating. *J. Atmos. Sci.*, **40,** 1897–1915.

Madden, R. A., 1986: Seasonal variations of the 40–50 day oscillation in the tropics. *J. Atmos. Sci.*, **43,** 3138–3158.

——, and P. R. Julian, 1971: Detection of a 40–50 day oscillation in the zonal wind in the tropical Pacific. *J. Atmos. Sci.*, **28,** 702–708.

——, and ——, 1972: Description of global scale circulation cells in the tropics with a 40–50 day period. *J. Atmos. Sci.*, **29,** 1109–1123.

Murakami, T., and T. Nakazawa, 1985: Tropical 45 day oscillation during the 1979 Northern Hemisphere summer. *J. Atmos. Sci.*, **42,** 1107–1122.

Sardeshmukh, P. D., and I. M. Held, 1984: The vorticity balance in the tropical upper troposphere of a general circulation model. *J. Atmos. Sci.*, **41,** 768–778.

Stevens, D. E., and G. H. White, 1979: Comments on "Viscous internal gravity waves and low-frequency oscillations in the tropics." *J. Atmos. Sci.*, **36,** 545–546.

Yamagata, T., and Y. Hayashi, 1984: A simple diagnostic model for the 30–50 day oscillation in the tropics. *J. Meteor. Soc. Japan,* **62,** 709–717.

Yasunari, T., 1980: A quasi-stationary appearance of 30 to 40 day period in the cloudiness fluctuations during the summer monsoon over India. *J. Meteor. Soc. Japan,* **58,** 225–229.

——, 1981: Structure of an Indian summer monsoon system with around 40-day period. *J. Meteor. Soc. Japan,* **59,** 336–354.